



CHAPTER IV

EFFECTS OF PYROLYSIS TEMPERATURES AND Pt-LOADED CATALYSTS ON POLAR-AROMATIC CONTENT IN TIRE-DERIVED OIL

4.1 Abstract

This study investigates the influences of pyrolysis temperatures and Pt-supported catalysts on polar-aromatic content in the oils obtained from pyrolysis of waste tire. These polar-aromatic compounds are mostly the sulfur-containing aromatics since oxygen is prohibited in pyrolysis. The experimental results indicated that pyrolysis temperatures strongly affected the polar-aromatic content in the derived oils. Namely, the increase in pyrolysis temperature in the tested range produced not only a higher amount of polar-aromatics but also heavier polar-aromatic compounds. All studied catalysts decreased the polar-aromatic content in the oils drastically. In addition, it was found that the introduction of the studied catalyst also led to the production of lighter polar-aromatic compounds with respect to that produced from thermal pyrolysis. Comparing the two acid catalysts, HBETA exhibited higher activity for polar-aromatic reduction as compared to HMOR, which was ascribed to its higher medium and strong acid site density, smaller particle size and 3D-structure. The Pt supported on HMOR and HBETA catalysts showed better polar-aromatic reduction activity than their corresponding acid catalysts. And, a slightly higher catalytic activity was observed over Pt/HBETA than Pt/HMOR, which was mainly due the higher Pt dispersion of Pt/HBETA catalyst.

4.2 Introduction

The world production of waste tires is approximately 5×10^6 tons/year and nearly 65–70% of these wastes are eventually legally or illegally land-filled [1,2]. Along the years, different alternatives for waste tire recycling such as retreading, reclaiming, incineration, and grindings have been used. However, all of them have many drawbacks and/or limitations. Pyrolysis of waste tire might be considered as a

non-conventional treatment, which recently has been received renewed attention and attempts, since it can produce some high valuable products such as oil and petrochemicals.

Polar-aromatic compounds are the aromatic substances containing a sulfur, oxygen, or nitrogen atom in aromatic rings. And, in tire pyrolysis, most of polar-aromatics are obtained in the liquid product, and believed to be mostly sulfur-containing aromatics as oxygen is prohibited in pyrolysis. In the tire structure, after vulcanization sulfur is located at the allylic positions [3], and these sulfur atoms might be present as mono-sulfide, cyclic-sulfide or even dependent sulfide [4]. Jitkarnka *et al.* showed that the breakdown of a tire molecule was initialized by breaking S - S bonds, and then spread out along the chains [5]. Nowadays, there has been a great interest in studying on polar-aromatics, for instance aromatic-type sulfur-compounds, in fuels since some of them have been proven to be carcinogenic [6] and mutagenic [7], and may also give rise to toxic and corrosive SO_x in the exhaust streams of combustion plant using such fuels [8]. In refinery, sulfur-containing compounds are removed from fuels by hydrotreating or hydrodesulfurization process (HDS). Nevertheless, understanding how polar-aromatics are formed in the pyrolysis of waste tire helps finding the ways to prevent their formation and/or to eliminate them during pyrolysis. Williams and Bottrill [8] in 1995 studied the sulfur-polycyclic aromatic hydrocarbons in tire pyrolysis oil and reported the presence of a large number of sulfur-containing polycyclic aromatic hydrocarbons (HCs). Furthermore, Pakdel *et al.* [9] found thiophene derivatives in the liquid products obtained from tire pyrolysis. Several attempts to study the effects of waste tire pyrolysis conditions on the sulfur content in the products have been reported. In the study of Diez *et al.* in 2004 [10], it was found that the amount of sulfur liberated in the liquid and gas fractions after the pyrolysis process was greater as the final temperature rose. Moreover, they also reported that the presence of chlorine in the liquid and gas products was negligible, regardless of the final temperature of pyrolysis. The production of sulfur-containing polycyclic hydrocarbons in the pyrolytic oil was believed to occur via the Diels - Alders reaction involving poly-cyclic aromatic hydrocarbon and sulfur [8].

Attempts have been made toward understanding the mechanism of the

thermal degradation of different tire components. In many cases, the outcomes were what one may have expected. For examples, the β -scission was found to be more preferable during the pyrolysis of natural rubber [11], polybutadiene [12], and styrene-butadiene rubber [13]. Corma *et al.* [14] reported the ability of acid zeolites for cracking mercaptans, thiophene and thiophene derivatives. The cracking of mercaptans might ultimately produce hydrogen sulfide and low molecular weight hydrocarbons. However, thiophenes and alkyl-thiophenes could hardly crack directly, but a prior partial saturation of the molecules *via* hydrogen transfer should give rise to cracking reactions. Moreover, most of the thiophenes converted mainly to coke, whereas the rest converted to gas and gasoline, but 2-methyl thiophene was more prompt to crack to give gas and gasoline. The high preference of thiophenes to convert into coke under cracking conditions was also reported in the study of Valla *et al.* [15].

Miguel *et al.* [16] found that the addition of acid catalysts did not affect the degradation temperature of the rubber, but it made a difference to the nature of the hydrocarbons obtained. They also reported that the greater the acidity was, the more aromatic hydrocarbons were produced. Platinum catalysts have been known as effective desulfurization catalysts [17], and noble metal catalysts are very active for hydrogenation reactions [18]. For deep HDS, the hydrogenating function of a catalyst is crucial because an initial hydrogenation of the refractory sulfur-containing molecules was found to reduce steric effects that impede the direct elimination of sulfur heteroatoms [19,20]. The known poisoning effect of Pt-based catalysts caused by the presence of sulfur-containing compounds in the feed might be overcome by the increase in the support acidity [21-25]. Moreover, in 2004, Santikunaporn *et al.* investigated the ring-opening of decalin and tetralin on HY and Pt/HY zeolite catalysts [26] and found that the production of ring-opening products was increased with the addition of Pt metal.

To our knowledge, there has been no research having conducted to study the effect of pyrolysis temperature and catalysts on the polar-aromatic content in tire-derived oil. Thus, the purposes of this work were to study polar-aromatic formation in the pyrolytic oil obtained from the non-catalytic pyrolysis of waste tire at various temperatures, and to investigate the distinctive effects of Pt-supported HMOR and

Pt-supported HBETA catalysts on the polar-aromatic formation.

4.3 Experimental

4.3.1 Catalyst Preparation

Two zeolites, mordenite (MOR, H-form, Si:Al = 19) and BETA (NH₄-form, Si:Al = 27) supplied by the TOSOH Company (Singapore) were first calcined in air at 500°C and 600°C, respectively, with a heating rate of 5 °C/min for 3 hours. Then, they were loaded with Pt using the incipient wetness impregnation technique to obtain 1 %wt Pt-supported catalysts. After that, the samples were pelletized, ground, and then sieved to a specific particle sizes of 400–425 μm. Finally, all catalysts were calcined in a flow of air at 500°C for 3 hours. Prior to catalytic activity measurement, the catalysts were reduced at 400°C by H₂ for 3 hours.

4.3.2 Catalyst Characterization

XRD patterns were obtained using the Rigaku D/Max 2200H using CuKα small radiation, and operated at 40 KV and 30 mA. The catalyst samples were scanned from 5° to 60° (2θ/θ) with a scanning speed of 5°/min. Hydrogen chemisorption was carried out using a conventional laboratory made-up system equipped with a TCD detector. Prior to performing the chemisorption at room temperature, an approximate 50 mg of sample was reduced using 5% hydrogen in nitrogen at the temperatures ramped up from room temperature to 800°C with a heating rate of 10°C/min. Temperature program desorption (TPD) using NH₃ was carried out in a TPD/TPR Micromeritics 2900 apparatus. Approximately 0.1g of sample was first pretreated in He at 550°C for 30 minutes. Then, the system was cooled to 100°C, and the NH₃ adsorption was performed using NH₃/N₂ for 1.5 hours followed by the introduction of He to remove the physically adsorbed NH₃ for 30 minutes at 100°C. Finally, the system was cooled to 50°C, and then the temperature program desorption was started from 50°C to 600°C with a heating rate of 5°C/min. The composition of the bifunctional catalysts was determined by Inductively Coupled Plasma (ICP) technique using a Perkin Elmer Optima 4300 PV machine after the dissolution of the catalysts. The surface area and pore size of the studied catalysts were characterized by N₂ physical adsorption using the Sorptomatic 2900

equipment. The Dupont TGA 2590 equipped with a thermal analyzer 2000, heated from 30 to 800°C with the heating rate of 10°C/min was employed to study the amount of coke in the used catalysts.

4.3.3 Pyrolysis of Waste Tire

Figure 4.1 displays the experimental diagram. A tire sample was pyrolyzed in the lower zone of the reactor from room temperature to the final temperature of 500°C with the heating rate of 10°C/min. This pyrolysis zone was kept at the final temperature for 1 hour to ensure the total conversion of tire. The evolved products were carried by a 25 ml/min nitrogen flow to the upper zone, where was controlled at 350°C and packed with a catalyst. The obtained product was passed through an ice-salt condensing system containing 3 consecutive condensers in order to separate incondensable compounds from the liquid product. The solid and liquid products were weighed to determine the product distribution. The amount of gas was then determined by mass balance. The gas product collected in a Dual Valve Tedlar PVF bag purchased from Cole Parmer was analyzed by a GC, Agilent Technologies 6890 Network system, using an HP-PLOT Q column (300mm x 0.32 mm ID and 20 µm film thicknesses) and an FID detector. The liquid product was first dissolved in n-pentane with the ratio of 40:1 to precipitate asphaltene prior to the determination of polar-aromatic content by liquid adsorption chromatography. Saturated hydrocarbons, mono-, di-, poly-, and polar-aromatics in the obtained maltenes were fractionated by means of the liquid adsorption chromatography technique reported in details elsewhere [27]. Only polar-aromatic fraction was brought to analysis in this study. Finally, a Varian CP 3800 Simulated Distillation Gas Chromatograph equipped with FID and a 15m x 0.25mm x 0.25 µm WCOT fused silica capillary column (SIMDIST GC) was used to analyze the polar-aromatic fractions, according to the ASTM D2887 method, for simulated true boiling point curves and carbon number distribution. From the obtained true boiling point curve, a polar-aromatic portion was cut into ranges as follows: gasoline (<149°C), kerosene (149 – 232°C), gas oil or diesel (232 – 343°C), light vacuum gas oil or fuel oil (343 – 371°C), and heavy vacuum gas oil (>371°C).

4.4 Results and Discussion

4.4.1 Catalyst Characterization

The XRD patterns of the Pt-supported catalysts and their corresponding supports are displayed in Figures 4.2a and 4.2b. These patterns indicate that the introduction of Pt to the zeolites did not affect the structure of the zeolites. However, due to the low amount of metal loaded on the catalysts, the peaks of Pt located at the 2θ of 39° and 46° [28] are then very small.

Figure 4.3 illustrates the TPD-NH₃ profiles of HMOR and HBETA. Both profiles have two peaks. In the profile of HMOR, the taller peak appears at the temperature of around 190°C , whereas the shorter peak locates at approximately 480°C . For HBETA, the first peak is observed at around 290°C and the second one is emerged at the temperature of 480°C . Obviously, according to the area under the peaks, HMOR possesses greater acid density than HBETA due to its lower Si:Al ratio. Meanwhile, the profile of HBETA exhibits the long-tail end, which is the characteristic of this zeolite [29]. In addition, TPD-NH₃ curve of HBETA shows higher amount of medium and strong acid sites (located at temperatures higher than 250°C), as compared to that of HMOR. This higher medium and strong acid site density might be attributed to the dislodged Al of HBETA [29]. Moreover, it should be noted that, in this study, HBETA was pretreated by calcination at the higher temperature as compared to HMOR. This probably increases the amount of dislodged Al [30], resulting in the higher medium and strong acidic sites of HBETA as observed from ammonia desorption spectrum.

For all used catalysts, the TG results show two different weight loss positions corresponding to two different types of deposited hydrocarbons. The first one is observed at a lower temperature of around 290°C , whereas the second one is located at around 500°C . Between the two studied zeolites, the higher amount of coke was observed on HBETA, possibly due to its larger pore volume (Table 4.1). And, the amount of coke produced on Pt/HMOR and Pt/HBETA is comparable but this amount is higher than that produced on their corresponding acid catalysts.

Table 4.1 Physical-chemical properties of studied catalysts

Catalyst	Pt %wt	Dispersion (%) ^a	Surface area (m ² /g)	Pore diameter (Å)	Pore volume (cm ³ /g)	Particle size (μm) ^d	Coke (g/g cat)
HMOR	-	-	372.5 ± 9.3	6.3 ^b	0.20 ^b	10-12	0.14
HBETA	-	-	618.3	7.5	0.68	3-6	0.22
Pt/HMOR	0.94	30.8	359.8	6.1	0.18	-	0.38
Pt/HBETA	1.01	42.1	608.5	7.1	0.67	-	0.33

^a Determined by H₂ chemisorption.

^b Determined by HK. method [31]

^d Supplied by TOSOH Corp.

The physical properties of the studied samples are also presented in Table 4.1. The amount of metal loaded was confirmed by using ICP technique. The obtained values of surface area of HMOR and HBETA samples displayed in the table are close to those supplied by the TOSOH, which are 380 and 630 m²/g, respectively. Moreover, clearly the introduction of Pt led to a decrease in both surface area and pore volume. The decrease in surface area and pore volume suggests the diffusion of Pt into the pore of the zeolites and/or the pore blockage. The hydrogen chemisorption results indicate that Pt is dispersed better on HBETA than on HMOR, possibly due to the higher surface area [32] of HBETA (Table 4.1). In addition, the slightly decrease in pore volume together with the higher amount of coke generated over Pt-supported catalysts and the H₂-chemisorption results suggest that a considerable amount of Pt is located outside the zeolite crystals.

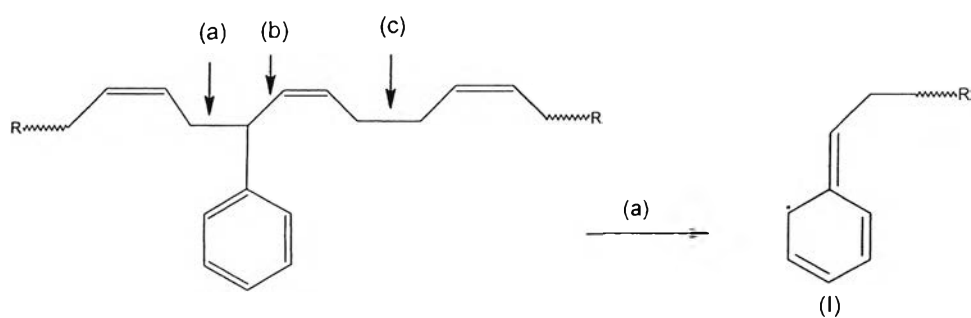
4.4.2 Polar-aromatic Formation in the Non-catalytic Pyrolysis of Waste Tire

Prior to being able to explain how the catalysts can help reducing polar-aromatic contents, the formation of such compounds needs to be understood. This section is contributed to the discussion about how polar-aromatics can be formed during the pyrolysis of waste tire.

4.4.2.1 *Polar-aromatic Formation from Thermal Cracking of Tire*

The chemistry of sulfur vulcanization is so complex that, even today, only the main stages have been proven. After vulcanization, sulfur was

combined in the network in a number of ways. Sulfur may be present as mono-sulfide, di-sulfide, or poly-sulfide, but it may also be present as dependent sulfides, or cyclic-mono- and cyclic-di-sulfides [4]. In addition, sulfur was found to attach to the rubber chains almost exclusively at the allylic positions [3]. Moreover, a typical tire compound contains natural rubber (NR), styrene butadiene rubber (SBR), poly butadiene and butyl rubber [33]. Therefore, the rubber chains of tire should contain the aromatic rings originally from SBR as well as double bonds. In addition, in the SBR, the configuration of styrene monomers could be both block and random. And, the amount of bound styrene (%wt) is in the range from 10 to 45% [3], depending on the way the SBR was synthesized.

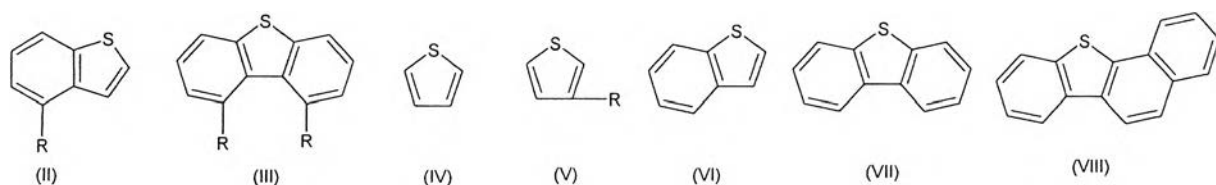


Scheme 4.1 All cracking positions on the SBR chain and the product **(I)** obtained from cracking at the most probable position **(a)** [13].

Several researches have investigated the thermal degradation of different rubbers. In the work of Chen and Qian [11], it was found that during the pyrolysis of natural rubber, β -scission was much more preferable because of the low bond dissociation energy, leaving the allylic radicals. The thermal cracking of polybutadiene also was reported to occur via β -scission [4]. Meanwhile, the thermal degradation of the styrene-butadiene rubber was favored to occur at the position **(a)** than at **(c)** in Scheme 4.1 as suggested by Choi [13], whereas no product resulting from the dissociation at the position **(b)** was observed. In addition, during the pyrolysis, not only the depolymerization but also the decomposition reaction to produce short chain hydrocarbon occurred [11].

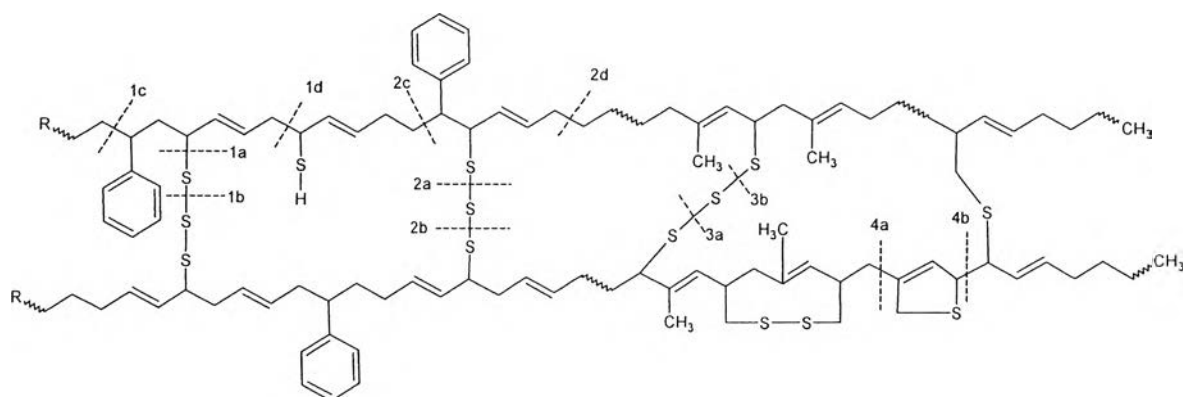
In the present study, it was found that the polar-aromatics

mainly distributed in the heavy fractions of the oils (light and heavy vacuum gas oils), which is in good agreement with some studies [9,34,35]. Scheme 4.2 shows several polar-aromatics found in the pyrolyzates from various references [9,34-36].



Scheme 4.2 Some polar-aromatics found in pyrolytic oils [9,34-36].

In order to ease the further discussion about polar-aromatic formation/reduction with respect to the pyrolysis conditions and the presence of catalysts, an example of tire structure is hereby anticipated, as shown in Scheme 4.3, based upon the earlier discussion on the possible cracking positions having been proposed to occur during the pyrolysis of waste tire [11-13] and upon our experimental results.

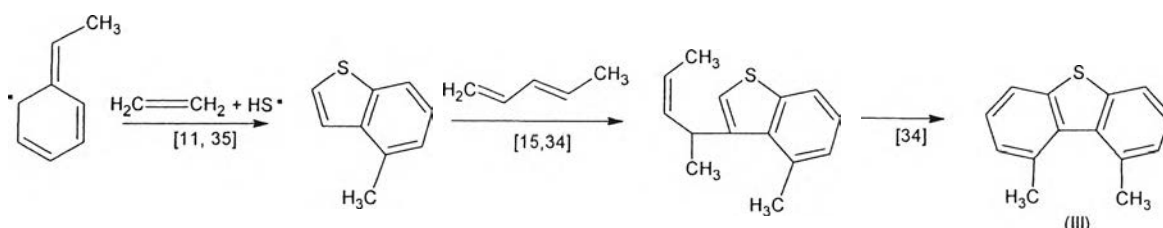


Scheme 4.3 A tire molecule (adapted from [4,8,33]) accompanied with the proposed possible cracking positions during pyrolysis [5,11-13].

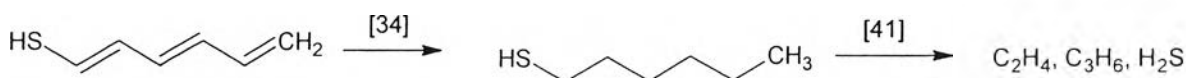
Sulfur, which is originally present in the tire rubber approximately by 1.7 %wt [37], is the source for the formation of sulfur-containing compounds during pyrolysis. In addition, oxygen is prohibited in pyrolysis.

Consequently, polar-aromatics found in pyrolysis oil are mostly sulfur-containing aromatics. In the study of Jitkarnka *et al.* [5], it was reported that the breakdown of a tire molecule would initially occur at the S-S bonds, and then spread out along the free rubber chains. According to the dissociation energy of the S-S, C-S, and C-C bonds, which are 429, 699 and 607 kJ.mol⁻¹, respectively [38], the free sulfur might easily be produced by the cracking of tire molecule at the positions **1a**, **1b**, **2a**, **2b**, **3a**, and **3b**.

The thermal cracking reaction could simultaneously occur at any position from **1** to **4**. The scissions occurring at the positions **1 a**, **b**, **c**, and **d** result in the formation of Species **(I)** [13] and some free sulfurs. After that, Species **(I)** might react with the generated free sulfurs under the presence of ethylene *via* the Diels–Alders reaction [8], followed by cyclization and dehydrogenation [35] to form **(II)**. Consequently, Species **(II)** further reacts with the produced olefins [34], and then again cyclizes yielding Species **(III)** as shown in Scheme 4.4.



Scheme 4.4 An example of polar aromatic formation via a consecutive reaction with free sulfurs.



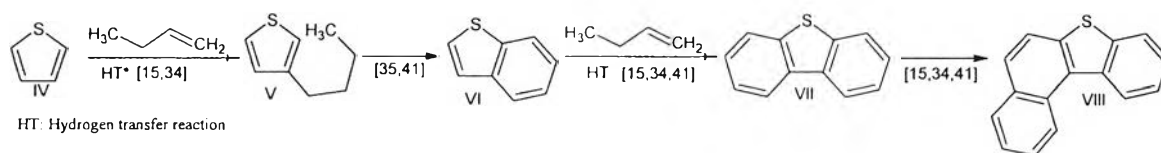
Scheme 4.5 An example of hydrogen sulfide production via hydrogenation followed by cracking.

The production of hydrogen sulfide [39,40] in the gas product could be explained by the reactions displayed in Scheme 4.5. Initialized by the simultaneous cracking of tire molecule at positions **1d** and **2c** in Scheme 4.3, the

product could then be stabilized by hydrogen coming from potential H-donor structures [34], followed by cracking to produce hydrogen sulfide and light olefins such as ethylene and propylene [41].

In contrast, with the presence of potential H-donor compounds during the pyrolysis [34], the produced H₂S might be added to the olefins generated by the thermal cracking to form thiols, which suffer the cyclization and dehydrogenation into thiophenic compounds [42,43].

The cracking of the rubber chain at the positions **2a**, **b**, **c** and **d** followed by the free radical stabilization and the cyclization reaction on the chain [44] could lead to the formation of alkyl benzothiophene (**II**). Moreover, thiophene could be directly produced via the cracking reaction at positions 4a and 4b, might undergo hydrogen transfer reaction [34]. The obtained product subsequently reacts with the available olefins [15,44], followed by cyclization and dehydrogenation [34], generating benzothiophene (V). Further reaction could also occur, leading to the formation of polycyclic polar-aromatic compounds, VIII, as shown in Scheme 4.6.



Scheme 4.6 An example of polycyclic polar-aromatic formation initialized by the direct cracking of tire.

4.4.2.2 Effect of Temperature on Polar-aromatic Production

The effect of pyrolysis temperature on polar-aromatic production was also investigated in the present study. The results show that under the pyrolysis temperature of 500°C, the amount of polar-aromatics account for approximately 11%wt of the obtained oil product. And, when the pyrolysis temperature increased, the amount of polar-aromatics increased (Figure 4.4).

From the results, it can be explained that at higher temperatures, more free radicals are generated at a greater rate, so many of them combine one another. As a consequence, more aliphatic chains linked to polar

aromatic structures as in Scheme 4.4, and then these chains might undergo cyclization reactions resulting in the production of much heavier polar-aromatic hydrocarbons as in Scheme 4.6. The decrement of gas product as observed in Figure 4.4 is also the consequence of the poly-aromatic formations. The shift of the peak to the higher carbon number with temperature shown in Figure 4.5 can be the evidence confirming the formation of bigger size poly-aromatic compounds in the oil products.

In summary, the formation of polar-aromatics could mainly be attributed to (i) the combinations of available olefins and free sulfurs, (ii) the combination of sulfur containing compounds with olefins, via the Diels–Alders reactions, and (iii) the direct cracking of tire molecule at where the S atoms are resided. Therefore, in order to reduce polar-aromatics in the pyrolytic oils without the introduction of hydrogen, one can either prevent them from formation via such means or force them by any mean to crack into lower molecules and eventually to hydrogen sulfide as in Scheme 4.5.

4.4.3 Effects of the Catalysts

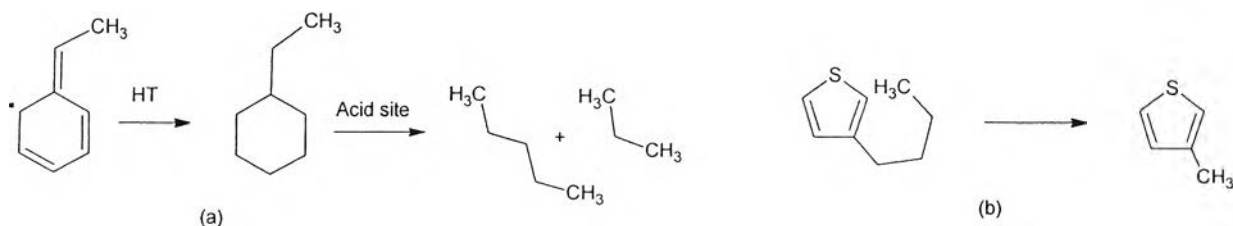
Figure 4.6 shows the percentages of the polar-aromatics in the pyrolytic oils obtained from the experiments run with different catalysts. From the figure, it is clear that HMOR and HBETA zeolites help decrease the amount of polar-aromatics by approximately 30%wt and 50%wt, respectively, as compared to the non catalytic case. The introduction of Pt on the zeolites led to a further decrease in the content of polar-aromatics. And, the lowest polar-aromatic content is observed when Pt/HBETA catalyst was used.

Figure 4.7 shows the simulated distillation of the obtained polar-aromatic portions, which were cut, according to the boiling points, into gasoline (<149 °C), kerosene (149–232 °C), gas oil or diesel (232–343 °C), light vacuum gas oil or fuel oil (343–371 °C), and heavy vacuum gas oil (>371 °C). According to the figure, one can see that polar-aromatics from the non-catalytic pyrolysis are mainly distributed in the range of gas oil and vacuum gas oil. The introduction of the catalysts alters the distribution of polar-aromatics to a range of lighter fractions. Especially, when the bifunctional catalysts were used, polar-aromatic compounds in the HVGO range are decreased remarkably. And, polar-aromatics are highly distributed in the kerosene range, instead of the gas oil range as having occurred

when the corresponding zeolites were used. Besides, a small amount of polar-aromatics in the gasoline range is obtained in the case of HBETA. This might be attributed to the fact that HBETA has two channels $7.6 \times 6.4 \text{ \AA}$ in diameter, and a third channel that is only $5.5 \times 5.5 \text{ \AA}$ wide [16], so that deep cracking of polar-aromatics might have occurred producing H_2S and light hydrocarbons in the gaseous product.

Figure 4.8 shows the shift of carbon number distribution of polar-aromatics to lower carbon numbers in conjunction with the narrower distribution when the catalysts were used. Many studies have proven that acid catalysts are able to crack thiophene, benzothiophene, and their derivatives to lower molecular weight substances [15,45]. Once polar-aromatics are formed, acid catalysts can crack them into smaller molecules, and possibly open aromatic rings, consequently reducing the total amount of the polar-aromatics in the pyrolytic oil.

As presented in this work, among the two zeolites, HBETA exhibits higher activity than HMOR in reducing the size of polar-aromatics as illustrated by the lower average carbon number (Figure 4.8) as well as the quantity of the compounds (Figure 4.6). The higher activity of HBETA as compared to HMOR might be attributed to its better cracking activity caused by the combination effects of its higher total amount of medium and strong acid sites (Figure 4.3), its smaller crystalline (Table 4.1), and especially its large sinusoidal pore systems [46,47]. Moreover, its larger pore diameter favors the diffusion of larger molecules into inner pores; thus, a higher amount of reactants including polar-aromatics might be cracked to smaller compounds.



Scheme 4.7 Examples of polar-aromatic reduction by acid catalysts [14,15].

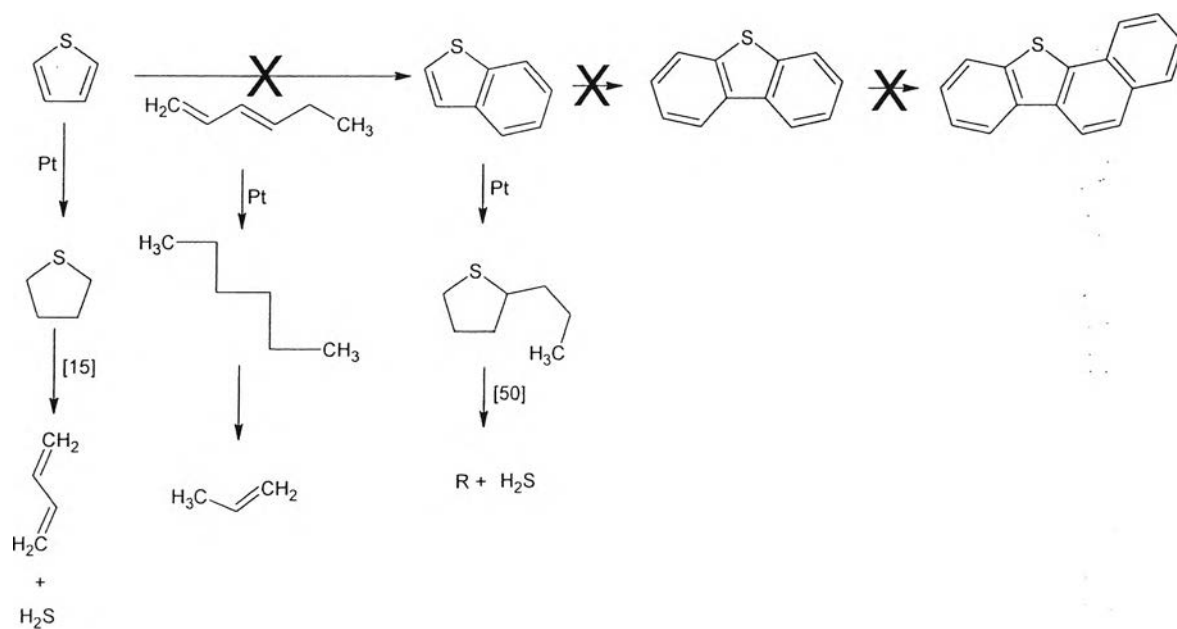
Additionally, it was reported that acid catalysts displayed the activity not only on the cracking polar-aromatics or sulfur-containing compounds, but also

on the cracking of a hydrogenated aromatic intermediate, as in Scheme 4.7a [14]. Prior to being converted to a polar-aromatic compound, Species (I) might be stabilized and cracked to produce lighter HCs, preventing the reactions in Scheme 4.6 from occurring. In addition, the presence of acid catalysts was found to convert long chain alkyl-thiophenes to shorter alkyl-thiophenes by cracking the alkyl chain of the former [14,15] as shown in Scheme 4.7b, resulting in the prevention of the formation of Species (VI) from (V) as illustrated in Scheme 4.6.

Table 4.1 has shown that HBETA forms the higher amount of coke than HMOR. This could be attributed to the higher total amount of medium and strong acid sites, and particularly its larger pore volume that favors the condensation of an aromatic compound to form coke [48]. Corma and his colleagues [14] also suggested a possible pathway to form coke from alkyl-benzothiophenes (Species II). In addition, the highest amount of coke is produced when the bifunctional catalysts were used, suggesting that possibly polar-aromatics are partially diminished by the formation of coke instead.

As shown in Scheme 4.4, the formation of polar-aromatics involves the interaction with accessible olefins. Consequently, if a catalyst can help eliminating these compounds, the polar-aromatic formation can be prevented. And, interestingly, that was indeed the case when the bifunctional catalysts were used. Although the HBETA zeolite alone displays much higher polar-aromatic reduction than the HMOR zeolite does (Figure 4.6); with the introduction of Pt, the polar-aromatic reduction activity of the two emerged bifunctional catalysts is found comparable. Consequently, the presence of Pt on the surface of the catalyst results in the prevention of polar-aromatic formation. This could be attributed to the high hydrogenation activity of Pt [18,49] that helps converting olefins and other unsaturated intermediates to saturated HCs, instead of being combined with one another to form heavier polycyclic polar-aromatic compounds as in Scheme 4.6. In addition, these hydrogenated compounds might further undergo cracking reactions, and then, are converted into lighter polar-aromatics or sulfur-containing compounds or even into H₂S in association with the formation of short-chain hydrocarbons. That explains the shift of the peak to the lower carbon number (Figure 4.7) when Pt-supported catalysts were present. Therefore, it is possible that the rate of the

hydrogenation catalyzed by Pt metal is faster than the rate of the combination reaction (as in Scheme 4.6 to yield heavier polar-aromatic compounds), leading to the reduction of polar-aromatic compounds in the pyrolytic oils. To visualize the previous explanation, Scheme 4.8 gives some examples of the prevented and favored reactions if thiophene, reported as a sulfur compound among other thiophene compounds found tire-derived oil [9,32-34], is present with the catalyst. Furthermore, as mentioned earlier, the polar-aromatic reduction activity of Pt/HBETA was slightly higher than Pt/HMOR. This could be attributed to the higher surface area of HBETA (Table 4.1), resulting in the better dispersion of Pt (Table 4.1) [32], and leading to a better hydrogenation activity.



Scheme 4.8 Some prevented and favored reactions by the bifunctional catalysts.

Finally, the bifunctional catalysts can also decrease the amount of polar-aromatics in the pyrolytic oil via the cracking reactions. Once polar-aromatics are formed, they might be hydrogenated on the Pt sites, followed by cracking on the acid sites, [50,51].

4.5 Conclusions

The complex structure of the tire makes it difficult to understand the multi-reactions occurring under the pyrolysis. In this study, the polar-aromatic formation in the pyrolysis of waste tire has been proposed. And pyrolysis temperature was found to strongly influence polar-aromatic content in the derived oil. The increase in the pyrolysis temperature led to an increment of polar-aromatic content, and also a shift of polar-aromatic distribution to the higher carbon number. The use of acid zeolites decreased polar-aromatic content dramatically. And, HBETA showed higher polar-aromatic reduction activity as compared to HMOR, which was ascribed to its acidic properties, small crystal size and 3D-structure. Especially, the introduction of Pt on the zeolites led to a further decrease in the polar-aromatic content. Pt/HBETA showed a slightly higher polar-aromatic reduction activity as compared to its counterpart, Pt/HMOR, which was explained by its higher metal dispersion.

The major role of Pt was to enhance the hydrogenation reactions, resulting in the conversion of polar-aromatics and their precursors to saturated HCs. Consequently, these compounds might undergo the cracking reactions catalyzed by the acid function of the catalysts, thus reducing the amount of the polar-aromatics.

4.6 Acknowledgements

These following agencies are acknowledged for their mutual financial support: The Petroleum and Petrochemical Consortium, the Thailand Research Fund (TRF), the "*Syntheses and Applications of Organometallics*" Research Unit of Chulalongkorn University, and The Graduate Scholarship Program for Faculty Members from Neighboring Countries of Chulalongkorn University.

4.7 References

- [1] S. Boxiong, W. Chunfei, G. Binbin, W. Rui and Liangcai, *Appl. Catal. B*, 73 (2007), 150-157.
- [2] S. Galvagno, S. Casu, T. Casabianca, A. Calebrese, and G. Cornacchia,

- Waste management, 22 (2002) 917-923.
- [3] J.E. Mark, B. Erman, and F. Eirich, Science and technology of rubber, 2nd Edition, Academic Press, San Diego, 1994.
- [4] C.M. Blow and C. Hepburn, Rubber technology and manufacture, 2nd Edition, Butterworths, Norwich, 1982.
- [5] S. Jitkarnka, B. Chusaksri, P. Supaphol and R. Magaraphan, J. Anal. Appl. Pyrolysis 80 (2007) 269-276.
- [6] M. L. Lee, M. Novotny and K.D. Bartle, Analytical Chemistry of Polycyclic Aromatic Compounds, Academic Press, New York, 1981
- [7] R.A. Pelroy, D.L. Stewart, Y. Tominga, M. Iwao, R.N. Castle and M.L. Lee, Mutat. Res. 117 (1981) 31.
- [8] P.T. Williams and R.P. Bottrill, Fuel, 74 (1995) 736-742.
- [9] H. Pakdel, D.M. Pantea and C. Roy, J. Anal. Appl. Pyrolysis, 57 (2001) 91-107.
- [10] C. Diez, O. Martinez, L.F. Calvo, J. Cara and A. Moran, Waste Management, 24 (2004) 463-469.
- [11] F. Chen and J. Qian, Fuel 81 (2002) 2071-2077.
- [12] F.M. Uhl, M.A. McKinney, C.A. Wilkie, Polym. Degrad. Stab. 70 (2000) 417-424.
- [13] S. Choi, J. Anal. and Appl. Pyrolysis 55 (2000) 161-170.
- [14] A. Corma, C. Martínez, G. Ketley and G. Blair, Appl. Catal. A: General 208 (2001) 135-152.
- [15] J.A. Valla, A.A. Lappas, I.A. Vasalos, Appl. Catal. A: General 297 (2006) 90 - 101.
- [16] G.S. Miguel, J. Aguado, D.P. Serrano, and J.M. Escola, J.M., Appl. Catal B: Environmental, (2006), 209-219.
- [17] V.G. Baldovino-Medrano, S.A. Giraldo, and A. Centeno, Fuel 87 (2008) 1917 - 1926.
- [18] M.F. Williams, B. Fonfé, C. Woltza, A. Jentys, J.A.R. van Veen, and J.A. Lercher, J. Catal. 251 (2007) 497-506.
- [19] J.B. McKinley, In: Emmett PH, editor. Catalysis, vol. 5. New York: Reinhold, 1957.

- [20] T.A. Pecoraro and R.R Chianelli, *J. Catal* 67 (1981) 430 – 445.
- [21] A. Stanislaus and B.H. Cooper, *Catal Rev-Sci Eng*, 36 (1994) 75 – 123.
- [22] H. Du, C. Fairbridge, H. Yang and Z. Ring, *Appl Catal A: Gen*, 294 (2005) 1 – 21.
- [23] H. Yasuda and Y. Yoshimura, *Catal Lett*, 46 (1997) 43.
- [24] N. Matsubayashi, H. Yasuda, M. Imamura and Y. Yoshimura, *Catal Today*, 45 (1998) 375.
- [25] R.M. Navarro, B. Pawelec, J.M Trejo, R. Mariscal and L.L.G. Fierro, *J. Catal.*, 189 (2000) 184.
- [26] M. Santikunaporn, J.E. Herrera, S. Jongpatiwut, D.E. Resasco, W.E. Alvarez and Ed L. Sughrue, *J. Catal*, 228 (2004), 100-113.
- [27] G. Sebor, J. Blaz ek, M.F. Nemer, *J. Chromatogr A*, 847 (1999), 323-330.
- [28] A.D. Schmitz, G. Bowers and C. Song, *Catal. Today*, 31 (1996) 45-56.
- [29] F. Lonyi, J. Valyon, *Thermochimica Acta* (2001) 53-57.
- [30] Y. Miyamoto, N. Katada, M. Niwa, *Micro. Meso. Mater.* 40 (2000) 271-281.
- [31] Horvath and Kawazoe, *J. Chem. Eng. Japan* 16 (1983) 47
- [32] C. Song and X. Ma, *Appl. Catal B: Environmental* 41 (2003) 207 – 239.
- [33] P.T. Williams and S. Besler, *Fuel* 14 (1995) 1277-1283.
- [34] I.M. Rodriguez, M.F. Laresgoiti, M.A. Cabrero, A. Torres, M.J. Chomón, B. Caballero, *Fuel Process. Techno* 72 (2001) 9 – 22.
- [35] M.F.Laresgoiti, B.M. Caballero, I.M. Rodriguez, A. Torres, M.A. Cabrero, M.J. Chomón, *J. Anal. Appl. Pyrolysis* 71 (2004) 917 – 934
- [36] K. Unapumnuk, T.C. Keener, M. Lu, F. Liang, *Fuel* 87 (2008) 951–956.
- [37] P.T. Williams and A.J. Brindle, *J. Anal. Appl. Pyrolysis* 62 (2003) 143-164.
- [38] J.A. Dean, *Lange's Handbook of Chemistry*, 15th Edition, McGrawHill, 1999.
- [39] D.Y.C. Leung, X.L. Yin, Z.L. Zhao, B.Y. Xu, Y. Chen, *Fuel Process. Techno* 79 (2002) 141– 155.
- [40] E. Aylon, R. Murillo, A. Fernandez-Colino, A. Aranda, T. Garcia, M.S. Callen, A.M. Mastral, *J. Anal. Appl. Pyrolysis* 79 (2007) 210-214.
- [41] X. Dupain, L.J. Rogier, E.D. Gamas, M. Makkee, J.A. Moulijn, *Appl. Catal. A: General* 238 (2003) 223 – 238.
- [42] P. Leflaive, J. L. Lemberon, G. Pérot, C. Mirgain, J. Y. Carriat and J. M.

- Colin, *Appl. Catal. A: General* 227 (2002) 201 – 215
- [43] H. Mizutani, Y. Korai and I. Mochida, *Fuel* 86 (2007) 2898 – 2905.
- [44] P.T. Williams and D.T. Taylor, *Fuel* 72 (1993) 1469-1474.
- [45] B. Li, W. Guo, S. Yuan, J. Hua, J. Wang, H. Jiao, *J. Catal.* 253 (2008) 212 – 220.
- [46] Yun Je Lee, Jong-Ho Kim, Seok Han Kim, Suk Bong Hong, Gon Seo, *Appl. Catal. B: Environmental* 83 (2008) 160-167;
- [47] A. Corma, J.Martinez-Triguero, and C. Martinez, *J. Catal.* 197 (2001), 151
- [48] D.Richardeau, G. Joly, C.Canaff, P. Magnoux, M. Guisnet, M. Thomas, A. Nicolaos, *Appl. Catal. A: General*, 263 (2004) 49-61.
- [49] A. Philippou and M.W. Anderson, *J. Catal.* 167 (1997) 266- 272.
- [50] F. Can, A. Travert, V. Ruaux, J.-P. Gilson, F. Maugéa, R. Hub, R.F. Wormsbecher, *J. Catal.* 249 (2007) 79–92.
- [51] R. Contreras, R. Cuevas-Garcia, J. Ramirez, L. Ruiz-Azuara, A. Gutierrez-Alejandre, I. Puente-Lee, P. Castillo-Viallalon and C. Salcedo-Luna, *Catal. Today* 130 (2008) 320 -326.

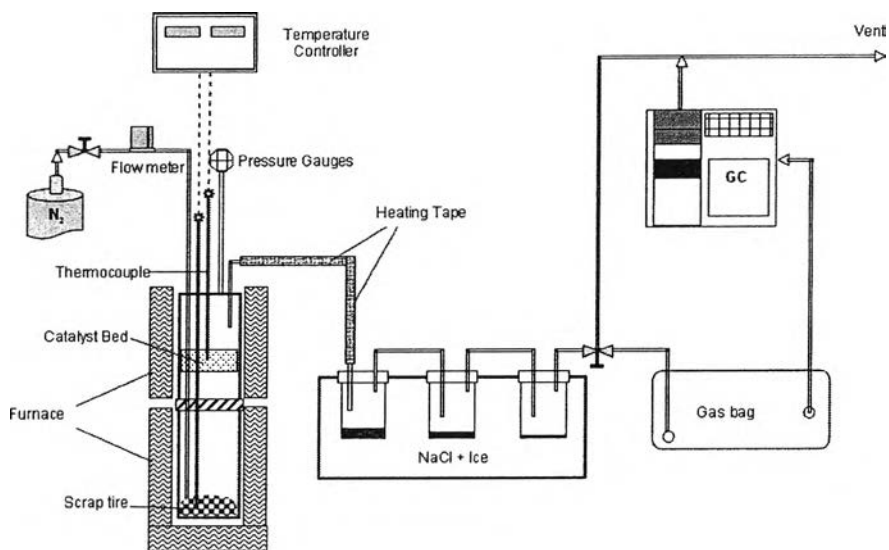


Figure 4.1 Schematic experimental system of waste tire pyrolysis

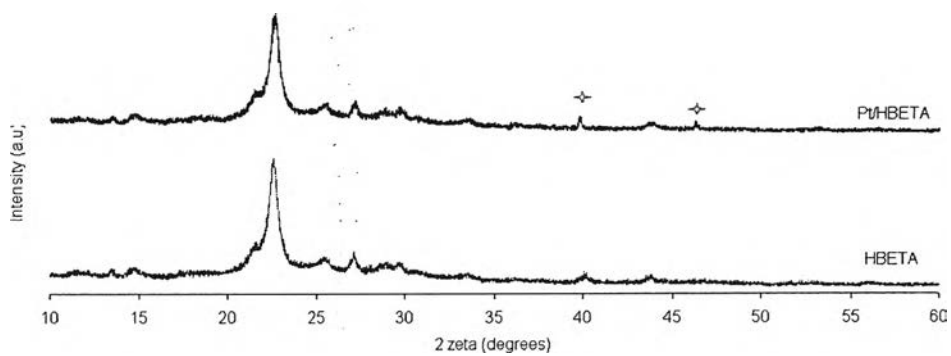


Figure 4.2a XRD patterns of HBETA and Pt/HBETA.

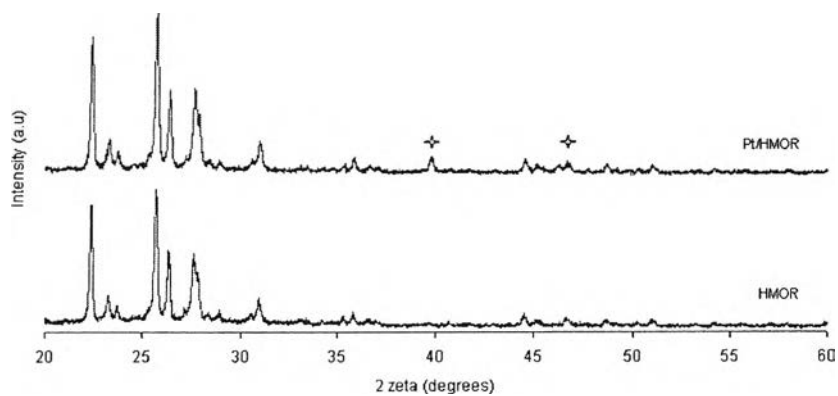


Figure 4.2b XRD patterns of HMOR and Pt/HMOR.

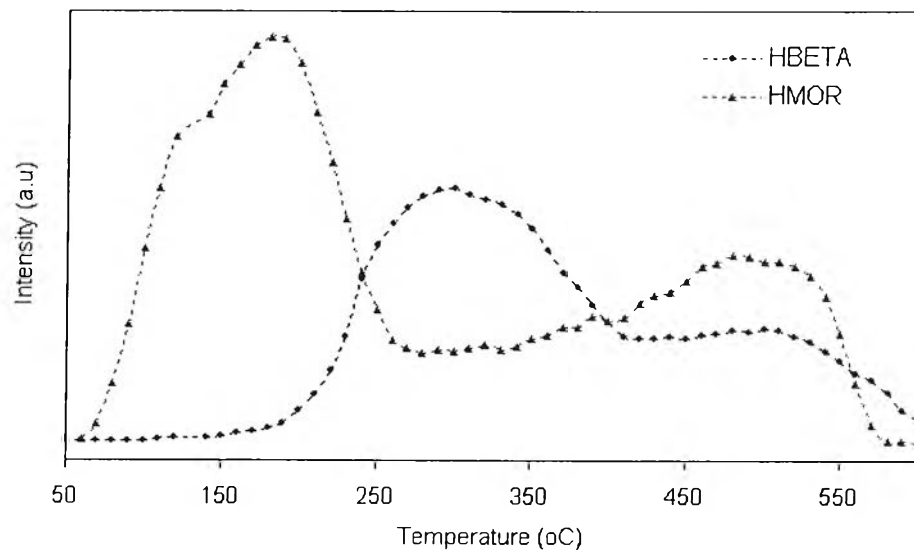


Figure 4.3 TPD-NH₃ of HBETA and HMOR.



Figure 4.4 Effect of pyrolysis temperature on the yield of polar-aromatics, gas, and liquid products.

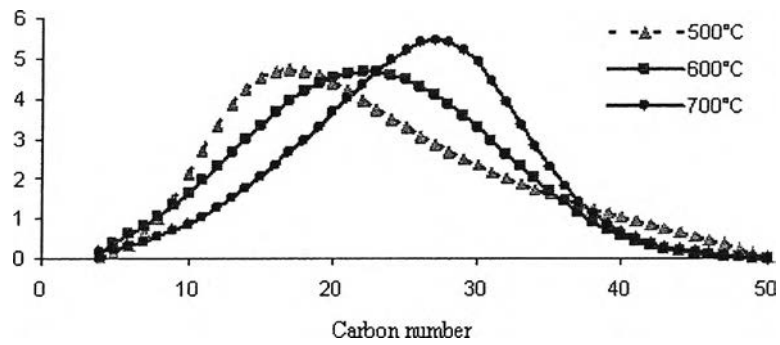


Figure 4.5 Effect of the final temperature on the carbon number distribution of polar-aromatic compounds.

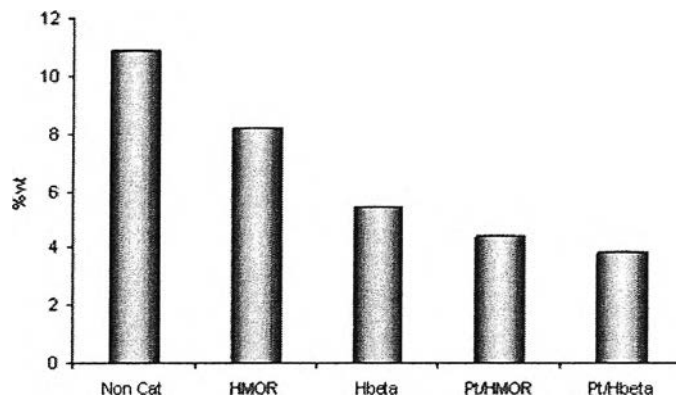


Figure 4.6 Effect of catalysts on the polar-aromatic content in the pyrolytic oils.

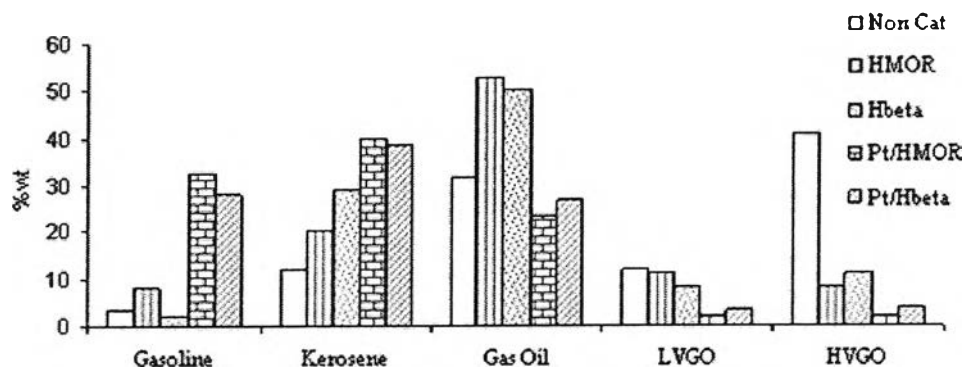


Figure 4.7 Effect of catalyst on polar-aromatic distribution.

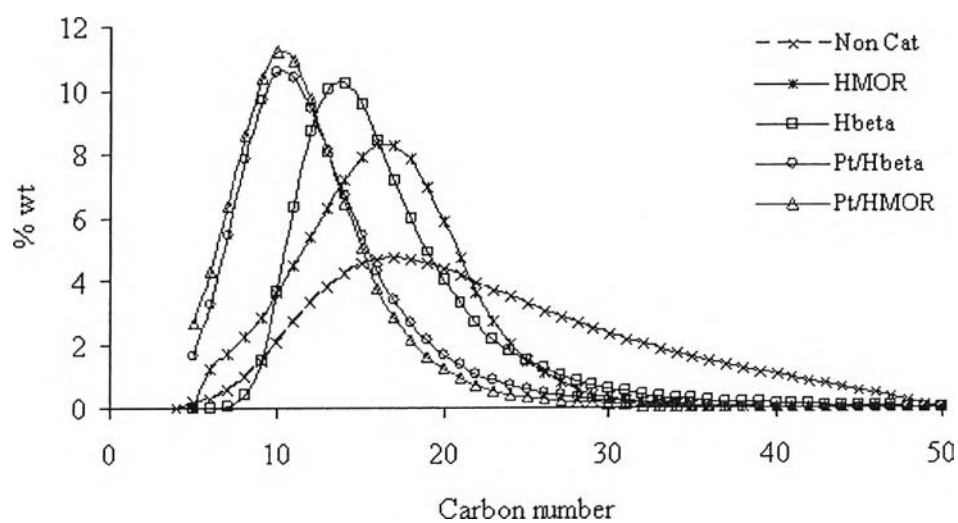


Figure 4.8 Effect of catalysts on the carbon number distribution of polar-aromatic compounds.